

# A New Coil Protection System for the Divertor Configuration at JET

V Marchese, J R Last, G Sannazzaro, L Scibile, J van Veen.

JET Joint Undertaking, Abingdon, Oxon, OX14 3EA.

"This document is intended for publication in the open literature. It is made available on the understanding that it may not be further circulated and extracts may not be published prior to publication of the original, without the consent of the Publications Officer, JET Joint Undertaking, Abingdon, Oxon, OX14 3EA, UK".

"Enquiries about Copyright and reproduction should be addressed to the Publications Officer, JET Joint Undertaking, Abingdon, Oxon, OX14 3EA".

# A New Coil Protection System for the Divertor Configuration at JET

V. Marchese, J.R. Last, G. Sannazzaro, L. Scibile, J. van Veen  
JET Joint Undertaking, Abingdon, Oxfordshire, OX14 3EA

## ABSTRACT

The paper describes a new Coil Protection System (CPS) which is planned to be installed at JET before the next experimental campaign with a pumped divertor. The protection system will make circuit equation integration, computations of forces on and stress in the coils and check current and voltage levels and coil heating effects in real time. If acceptable values for any of these parameters are exceeded, the pulse will be terminated. A fully digital implementation of the algorithms is being designed using a high performance Digital Signal Processor (DSP). A programme has been written for convenient off-line calculation and checks of model parameters with JET data.

## 1. INTRODUCTION

The new CPS will detect electrical faults and protect the coils against mechanical or thermal overstressing due to operation outside safe limits. The motivation for the new CPS comes mainly from the newly installed divertor coils [1]. The existing short circuit detectors for toroidal and poloidal coils, based on voltage comparison between coil subassemblies and ampere-turn measurements (Rogowski), are not feasible for the divertor coils because each one is different and there is no space to install current and voltage transducers in the vacuum vessel. In order to make the system completely independent from the control system, new voltage and current transducers have been installed in most of the circuits. The voltage measurements are used for overvoltage protection and also as inputs to the poloidal and toroidal circuit models. The circuit inductance and resistance matrices are preset on the basis of the magnetic configuration. The poloidal field model includes a correction to take into account the variation of the plasma with time and the effect of the iron core whilst unsaturated. The computed currents are compared with the measured currents. A large difference would indicate a possible fault, an open circuit or a configuration error and would terminate the pulse.

The radial and vertical forces on the outer poloidal coils P2, P3 and P4 [2] and the vertical forces on the divertor coils are computed via coil flux loops and ampere-turns. Since vertical flux loops have not been fitted on the divertor coils because of lack of space, the radial forces acting on these coils will be computed analytically. The tensile and shear stress of each coil, assuming a uniform distribution, is computed as a linear combination of vertical force, radial force and  $I^2t$ . The coefficients are determined by mechanical analysis. The detection of some possible faults specific to the magnetising coil P1 will also be implemented in the new system [3].

A simplified model will be used to estimate the temperatures of the epoxy insulation and copper windings of the divertor coils. The inputs to the model are the vessel temperature, the coils case temperature, the coil currents, the coolant flow and the coolant inlet and outlet temperatures.

## 2. FAULT DETECTION ALGORITHMS

### 2.1 POLOIDAL CIRCUIT

The poloidal field (PF) includes up to  $n=10$  independent circuits and up to  $m=22$  coil elements as listed in Table 1.

TABLE 1: Poloidal Circuit and Coil Elements

Circuit	Coil Elements	Power Supply
1 P1End	P1EU, P1EL, P3MU, P3ML	PFGC
2 P1 Centre	P1CU, P1CL	PFX
3 Radial Field	P2UIR, P2LIR, P3UR, P3LR	FRFA
4 Shaping Field	P2UOS, P2LOS, P2UIS, P2LIS P3US, P3LS	PSFA
5 Upper Vertical Field	P4UV	VFA1
6 Lower Vertical Field	P4LV	VFA2
7 Divertor Field 1	D1	PDFA1
8 Divertor Field 2	D2	PDFA2
9 Divertor Field 3	D3	PDFA3
10 Divertor Field 4	D4	PDFA4

Legend: E=End C=Central L=Lower R=Radial  
M=Magnetising I=Inner O=Outer S=Shaping

The circuit equations, in presence of a stationary plasma -  $I_p$  - (i.e., plasma centre in fixed position) are:

$$L_{\theta} \cdot \frac{dI_{\theta}}{dt} + R_{\theta} \cdot I_{\theta} = U_{\theta}$$

$$U_{\theta} = V_{\theta} - \left| L_{1p} \ L_{2p} \ \dots \ L_{np} \right|^T \cdot \frac{dI_p}{dt} \quad (1)$$

where:

$V_{\theta}$  (n) - vector of the input voltages,  $I_{\theta}$  (n) - vector of the computed PF circuit currents,  $L_{\theta}$  ( $n \times n$ ) - circuit inductance matrix,  $R_{\theta}$  ( $n \times n$ ) - circuit resistance matrix,  $L_{ip}$  - mutual inductance of the "i-th" circuit with the plasma.

The system inductance matrix, when the iron core is saturated, is computed as  $C \cdot \Lambda \cdot C^T$  where "C( $n \times m$ )" is the configuration matrix and " $\Lambda(m \times m)$ " is the coil single turn inductance matrix. The direction of the currents in each coil element is specified in the configuration matrix by means of the sign of the relevant number of turns ( $n_i$ ). The currents are assumed to be positive when flowing in anticlockwise as seen from the top of the machine.

The unsaturated state of the iron core has been modelled, as first approximation, by adding to each element (i, j) of the inductance matrix, the contributions  $N_i \cdot N_j \cdot L_o$ , with  $L_o = 10\mu H$  and  $N_i$  total number of turns in "i-th" circuit. The iron core is assumed to be saturated when the total ampere-turns of the poloidal system, (absolute value), exceeds 230 kAt. An improved model of the iron core based on the use of the limb flux loops will be defined at a later stage.

The plasma current derivative is calculated as the difference between the vessel un-integrated Rogowski coil signal and the divertor current derivatives:

$$\frac{dI_p}{dt} = \oint \frac{dH}{dt} dl - \sum_{i=7,10} \frac{dI_{\theta}(i)}{dt} \quad (2)$$

The small contribution of the vessel toroidal current is neglected. The divertor current derivatives are measured with pick-up coils designed at JET.

The smallest time constant of the system, in the usual configuration, is of the order of 100ms and therefore an integration time of 10ms appears to be adequate. The trapezoidal formula will be used as integration method.

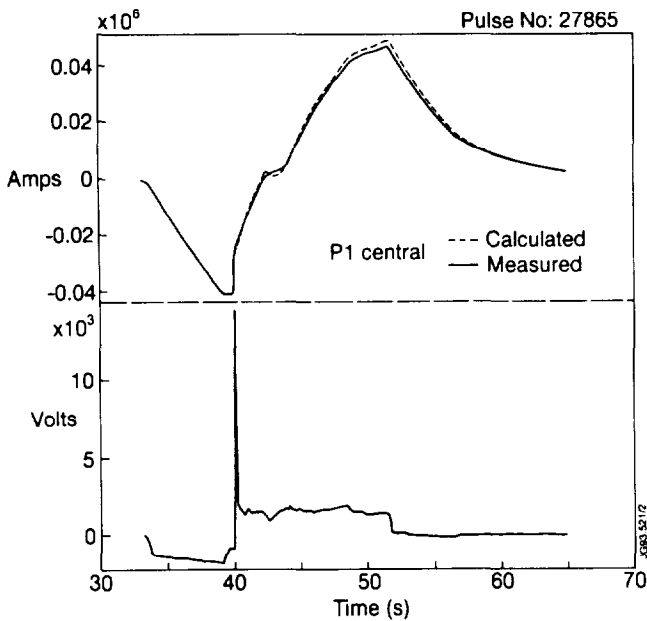


Fig. 1: PF Model-Comparison with JET data

Two sets of matrices of the associated sampled system will be used, the first for the unsaturated and the second for the saturated core case. The model outputs have been compared with JET experimental data (Pulse 27865) with good results (see Fig. 1).

## 2.2 TOROIDAL CIRCUIT

The toroidal field (TF) circuit includes the configuration for the "ripple" experiment. In this configuration the 32 D-shaped TF coils have been split into two sets. The odd coils (TC1) are fed from the Toroidal Flywheel Generator & Converter (TFGC) and even coils (TC2) are fed from two thyristor converter units (Static Unit 1 & 2) connected in series. Two first order, time varying, differential equations represent with sufficient accuracy the current transient in the two sets of coils:

$$L_{\phi} \cdot \frac{dI_{\phi}}{dt} + R_{\phi}(t) \cdot I_{\phi} = V_{\phi} \quad (3)$$

where  $V_{\phi}$  is the vector of the input voltages,  $I_{\phi}$  is the vector of the computed TF currents,  $R_{\phi}$  is the circuit resistance matrix (diagonal)  $L_{\phi}$  is the circuit inductance matrix (symmetric).  $R_{\phi}$  is a function of the temperature of the copper which, for the TF coils, changes considerably during a pulse. This is taken into account with the following equations:

$$R_{\phi}(t) = R_{\phi}(0) + \beta \cdot \int_0^t I_{\phi}^2(\xi) d\xi \quad (4)$$

The model has been tested on a 67kA pulse and has shown a very good agreement with the experimental data (see Fig. 2). The resistance of the entire TF coil before the pulse was 60mΩ and the coefficient  $\beta = 1.18e-13$ . The total self inductance was assumed to be constant at 0.64H.

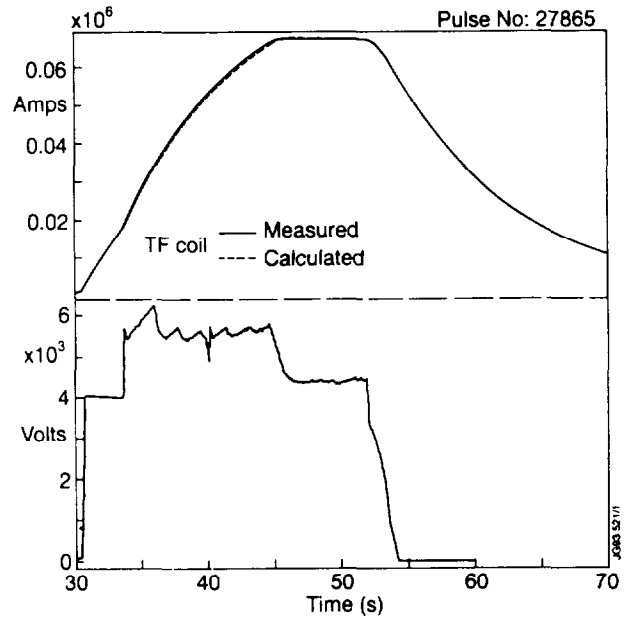


Fig. 2: TF Model-Comparison with JET data

Since the two time constants of the load are in the order of 5 seconds, the 10ms integration time as used for the PF model is more than adequate. Assuming the input voltage is constant over each time step, the circuit equations (3) and (4) will be integrated recursively using the Euler integration formula, thus avoiding matrix inversion at each step.

## 2.3 FORCES AND STRESSES

The stress parameters considered are the copper tensile stress ( $\sigma$ ) and the insulation shear stress ( $\tau$ ). These are given by equations of the form

$$\begin{aligned} \sigma &= aF_r + bF_z + cT \\ \tau &= dF_r + eF_z + fT \end{aligned} \quad (5)$$

where  $F_r$  and  $F_z$  are the radial and vertical forces per unit length acting on a coil,  $T$  is the temperature of the coil (computed from the energy dissipated),  $a$ ,  $b$ ,  $c$ ,  $d$ ,  $e$  and  $f$  are

coefficient related to the coil and obtained by mechanical analysis.

The radial and vertical forces acting on each coil element are given by equations of the form:

$$\begin{aligned} F_r &= nI B_z \\ F_z &= nI B_r \end{aligned} \quad (6)$$

where  $n$  is the number of turns on the coil,  $I$  is the current in the coil and  $B_z$  and  $B_r$  the measured fields crossing the coil. The total vertical force transmitted to the vacuum vessel by the divertor coils is the sum of the forces acting on the 4 coils

The vertical field at the divertor coils is not measured but will be estimated as a linear combination of the ampere-turns of all coils and the plasma current. The contribution of coil P1 can be neglected since almost all the flux is confined within the iron core.

The protection system also detects operation faults in the P1 circuit such as separating forces between coils [3] and inductive effects during disruptions.

## 2.4 DIVERTOR COIL THERMAL MODEL

During operation the temperature of the vessel is maintained at about 300 °C. This means that as long as the vessel is hot, the divertor coil cooling has to be continual.

In order to keep the epoxy resin in the main body of the coil below its glass transition temperature (about 75 °C) with some safety factor (say 25%) the temperature of the epoxy should be kept always below 60 °C. This is achieved into two ways:

- ◆ Limiting the maximum  $I^2t$  on the basis of the initial temperature of the coolant before the pulse
- ◆ Monitoring the coil case temperature during baking of the vessel.

The average epoxy and copper temperatures of the divertor coils will be estimated by considering heat inputs by radiation and conduction and by ohmic heating and cooling by Freon coolant. The inputs to the model are the vessel temperature ( $T_v$ ), the Freon coolant flow rate ( $q_f$ ), the coil case temperature ( $T_c$ ) and the coolant inlet and outlet temperatures ( $T_{in}$  and  $T_{out}$ ).

In order to reduce the thermal stresses between turns, the temperature difference ( $T_{out} - T_{in}$ ) has to be maintained below 20°C. This is achieved by recirculating the hot coolant from the outlet to the inlet circuit [4] and checked by CPS.

## 3. PROTECTIVE ACTIONS

The block diagram shown in Fig.3 summarises all the fault detection algorithms. Hardware faults within the protection system itself are not shown. Measurements or computed quantities are compared with suitable thresholds. If a threshold is exceeded an alarm is generated and protective actions are taken.

The circuit currents, the forces and the stresses on PF and divertor coils are computed only during "Pulse On", whilst the remaining quantities are monitored continuously.

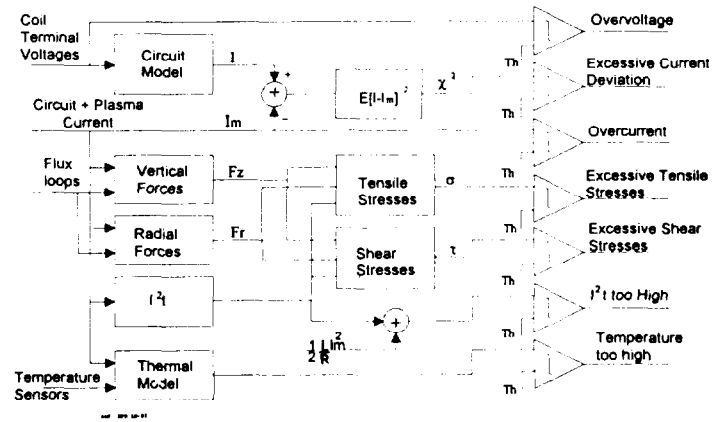


Fig. 3 Fault Detection Algorithms

A contribution  $(L / 2R)I_m^2$  is added to the  $I^2t$  to take into account the residual magnetic energy of the coil. The thresholds for the  $I^2t$  limits on the divertor coils will be computed as functions of the initial temperature of the coolant as follows:

$$(I^2t)_{max} = 0.46(60^\circ - T_{start}) \cdot 10^9 \quad (7)$$

Similar equations will be used also for the TF coil  $I^2t$  protection.

The new protection system will be interfaced with the following JET devices:

- PF and TF Power Supplies
- PF Crowbar
- Pulse Termination Network (PTN)
- Central Interlock and Safety System (CISS)
- Control and Data Acquisition System (CODAS)

Two fail-safe commands are sent individually to the PF and TF power supplies: a Voltage Off (VOF) and a Circuit Breaker Open (CBO) command (see Table 2).

The PF crowbar is closed if the "average" current of the magnetising coil P1, defined as  $(N_1 I_1 + N_2 I_2) / (N_1 + N_2)$ , exceeds the nominal value of 40kA by 10%.

These commands are backed-up by the actions performed via PTN and CISS. Two actions are required of PTN: the Slow Pulse Termination (SPT) and the Fast Pulse Termination (FPT). The SPT is defined as a controlled termination of the pulse (e.g. few seconds), via the Plasma Position & Current Controller (PPCC), and a staggered switching OFF of the plasma additional heating (ICRH, LHCD and NBI) thus avoiding disruptions. The FPT instead will remove the voltage from the coils and the additional heating as quickly as possible (e.g., it takes about 300ms to de-excite PFGC and TFGC). The actions required via CISS are Inhibit Pulse (IP) and Emergency Shutdown (ES).

All the alarms and statuses of the system will be transmitted to CODAS. Some protective actions that need to be implemented in a time of the order of a few minutes are left to the operator in the control room. For example, the switching off of the baking in case of an un-recoverable failure of the cooling system of one of the divertor coils when the vessel is hot (350°C).

TABLE 2: CPS Protective Actions

Circuit	Fault Detection Algorithm	Protective Actions					
		PS VOF	PS CBO	PTN SPT	PTN FPT	CISS IP	CISS ES
PF	Over voltage	x			x		x
	Excessive Current Deviation	x			x		x
	Overcurrent 5%	x			x		x
	Overcurrent 10%		x		x		x
	$I^2t$ too high	x			x		x
	Excessive Shear Stresses	x			x		x
	Excessive Tensile Stresses	x			x		x
Temperature too high				x		x	
TF	Over-voltage	x		x			x
	Excessive Current Deviation	x		x			x
	Overcurrent 5%	x		x			x
	Overcurrent 10%		x	x			x
$I^2t$ too high	x		x			x	

#### 4. IMPLEMENTATION

The heart of the system is a VME crate (see Fig. 4). Most of the modules are standard components and others have been designed by JET and manufactured by outside companies.

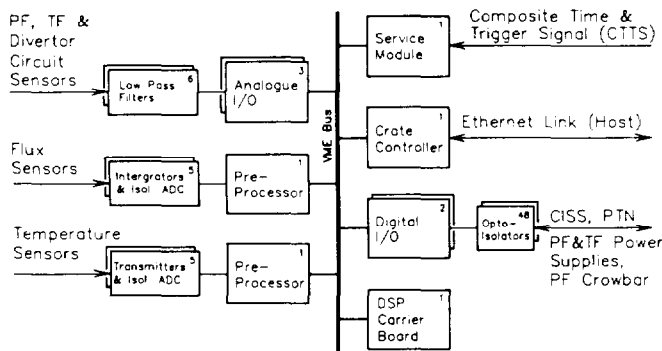


Fig. 4: CPS Hardware Configuration

The Service Module performs the function of synchronising all the internal timers to the Central Timing System by decoding the CTTS signal. This is an encoded signal containing a 1MHz clock, trigger signals and pulse parameters. It also performs subsidiary functions such as air-flow monitoring and checking the VME crate power supply for healthy status.

The VME crate is interfaced with the host computer by means of an Ethernet link via the Crate Controller fitted with

a Motorola 68040 processor clocked at 33MHz.

The Digital I/O is a standard board, fitted with a security watch-dog mechanism, which directly interfaces the VME bus. It provides 40 inputs and 32 outputs isolated in groups of 8 channels. The galvanic isolation of each channel with the outside world is performed with standard opto-isolators operating at 24V.

The DSP carrier board can accommodate up to two TIM modules each containing a Texas Instrument TMS320 C40 parallel DSP clocked at 40MHz. This incorporates a powerful floating-point processor and will be used to perform most of the fault detection algorithms described previously. The external interfaces also include two RS232 serial ports and the daisy-chained JTAG port for the two TIM modules.

The Analogue I/O card contains a 12 bit Analogue to Digital Converter (ADC) capable of sampling rates of up to 320kHz. The input multiplexers will be configured to provide 16 differential channels of analogue input all sampled at the maximum frequency of 10kHz.

The Pre-processor board contains a Motorola 68030 processor and it can handle up to 64 channels of analogue signals sampled at the maximum frequency of 10kHz. The Pre-processor will be used to perform drift compensation of the integrators, and conversion to engineering units.

The Software is being developed in two different environments: a PC based development system, with OS/2, for the DSP, and a X-Terminal, Operating under UNIX, for the 68k family processors.

The development and testing of the DSP software is based on the TMS320 Software Development Tools provided by Texas Instruments. The software is loaded into the C40 processor via the front panel JTAG connector. The majority of the code is written in 'C'.

Similar tools are available on X-Terminal for the 68k series processor running VxWorks. The software for the 68k family processors, including the communication with the host computer is common for most of the VME applications in JET. The X-Terminal is also used for the man-machine interface in the remote control room.

System simulations, calculations and comparison with the experimental data are performed with a dedicated computer code. The code will be used also for sensitivity analysis and as a convenient off-line simulator for the Coil Protection System.

#### REFERENCES

- [1] E. Bertolini and the JET team, "JET Development Towards Pumped Divertor Operations", this conference.
- [2] M. Huguet et al, "The JET Machine: Design, Construction and Operation of Major Systems", Fusion Technology, January 1987.
- [3] P.L. Mondino et al, "The PF System Enhancement in JET to produce plasma currents up to 7MA with material limiters and up to 4MA with magnetic separatrix: a report on electrical study", 12th SOFE conference, Monterey, U.S.A., 1987.
- [4] J.R. Last et al, "The JET Divertor Magnetic Configurations and Coil Design", 16th SOFT Conference, London, 1990.